New Phytologist

Research

Aging later but faster: how *StCDF1* regulates senescence in *Solanum tuberosum*

Li Shi[1], Laura de Biolley[1], Maroof Ahmed Shaikh[2], Michiel E. de Vries[3], Sybille Ursula Mittmann[4], Richard G. F. Visser[1], Salome Prat[2] and Christian W. B. Bachem[1]

[1]Plant Breeding, Wageningen University & Research, PO Box 386, Wageningen, 6700 AJ, the Netherlands; [2]Center for Research in Agriculture Genomics (CRAG), Barcelona, 08193, Spain; [3]Solynta, Dreijenlaan 2, 6703 HA, Wageningen, the Netherlands; [4]Aardevo B.V. Johannes Postweg 8, 8308 PB, Nagele, the Netherlands

Author for correspondence:
Christian W. B. Bachem
Email: christian.bachem@wur.nl

Received: *13 October 2023*
Accepted: *16 December 2023*

New Phytologist (2024)
doi: 10.1111/nph.19525

Key words: life cycle, senescence, *Solanum tuberosum*, *StCDF1*, *StORE1*, tuberization.

Summary

- In potato, maturity is assessed by leaf senescence, which, in turn, affects yield and tuber quality traits. Previously, we showed that the *CYCLING DOF FACTOR1* (*StCDF1*) locus controls leaf maturity in addition to the timing of tuberization. Here, we provide evidence that *StCDF1* controls senescence onset separately from senescence progression and the total life cycle duration.
- We used molecular–biological approaches (DNA-Affinity Purification Sequencing) to identify a direct downstream target of StCDF1, named *ORESARA1* (*StORE1S02*), which is a NAC transcription factor acting as a positive senescence regulator.
- By overexpressing *StORE1S02* in the long life cycle genotype, early onset of senescence was shown, but the total life cycle remained long. At the same time, *StORE1S02* knockdown lines have a delayed senescence onset. Furthermore, we show that StORE1 proteins play an indirect role in sugar transport from source to sink by regulating expression of *SWEET* sugar efflux transporters during leaf senescence.
- This study clarifies the important link between tuber formation and senescence and provides insight into the molecular regulatory network of potato leaf senescence onset. We propose a complex role of *StCDF1* in the regulation of potato plant senescence.

Introduction

Plant senescence is the last stage of plant development. During this period, structures and chemical compounds in the chloroplast are broken down allowing nutrients to be recycled and reallocated to other parts of the plant for storage or further development (Guiboileau *et al.*, 2010). This process includes leaf senescence, which is characterized by a decrease in chlorophyll content of leaves, discontinuation of meristem development, and degradation of macromolecules such as proteins and nucleic acids (Hörtensteiner, 2009). The senescence process has been well-studied in several plant systems as it is a critical trait which can influence yield and nutritional value (Woo *et al.*, 2018). Potato (*Solanum tuberosum*) is a member of the Solanaceae family and the most important nongrain food crop (Zaheer & Akhtar, 2016). Despite a long history of potato cultivation, several aspects of potato development and life cycle regulation remain elusive.

In many other crops, maturity refers to flowering time, seed maturity, fruit ripening and leaf senescence (TeKrony *et al.*, 1979; Maul *et al.*, 1998; Wang *et al.*, 2020). In potato, phenotyping underground development is difficult. Therefore, breeders focus mainly on phenotyping the aboveground leaf maturity, instead of tuber maturity. For potato, plant maturity is considered to be one of the most important genetically controlled, physiological components for phenotyping in breeding programs for predicted harvest timing and yield improvement (Wallace *et al.*, 1993; Prat, 2006). Maturity is generally scored on an ordinal scale from 1 to 7 with 1 being green plants and 7 being dead plants (Hurtado *et al.*, 2011). Furthermore, potato maturity is frequently evaluated by scoring only once, at a time point where the breeder observes the greatest variation in a population. Thus, the senescence onset, senescence progression speed and other senescence-related factors remain less well characterized.

Leaf maturity is affected by numerous internal and environmental cues. In potato, tuberization onset and leaf maturity are tightly linked physiologically and genetically. In fact, these two traits have often been mapped to the same genetic locus (Visker *et al.*, 2003; Kloosterman *et al.*, 2013; Jing *et al.*, 2022). A major-effect quantitative trait locus (QTL), located on chromosome 5, is responsible for foliage maturity, tuberization onset, and final potato yield (Visker *et al.*, 2003; Kloosterman *et al.*, 2013; J. Li *et al.*, 2019). This QTL was shown to be functionally linked to a DOF family gene (DNA-binding with one finger) coding for a transcription factor named CYCLING DOF FACTOR1 (StCDF1) that was found to regulate tuberization and plant life cycle length. In diploid potato, the genotypes with truncated variants have earlier leaf maturity. The truncated variants of StCDF1 exhibit enhanced protein stability caused by inability to

bind to GIGANTEA (StGI) and FLAVIN-BINDING, KELCH REPEAT, F-BOX (StFKF1) (Kloosterman *et al.*, 2013). Overexpressing truncated *StCDF1* (*StCDF1.2*) in the late tuberizing and late leaves maturing background (homozygous *StCDF1.1*) leads to both early tuberization and a short life cycle in potato (Kloosterman *et al.*, 2013). Furthermore, a study based on 6 tetraploid genomes demonstrated that the allelic variants of *StCDF1* correlate with leaf maturity in a dosage-dependent manner (Hoopes *et al.*, 2022). Recently, Jing *et al.* (2022) reported that the *StABI5-like 1* gene (*StABL1*) codes for a transcription factor which also positively influences tuberization onset and leaf senescence. In these studies, early tuberization was linked to the *FLOWERING LOCUS T-like* (*FT-like*) gene *SELF-PRUNING 6A* (*StSP6A*). StSP6A is a small globular protein that acts as a mobile tuberigen and belongs to the phosphatidylethanolamine-binding protein (PEBP) family (Navarro *et al.*, 2011; Zhang *et al.*, 2020). In stolon tips, StSP6A forms a tuberigen activation complex (TAC) with St14-3-3s and StFD-LIKE1 (StFDL1) to activate downstream tuberization-related genes (Teo *et al.*, 2017). Tuber formation requires assimilate translocation. StSP6A is also found to be involved in leaf-to-stolon sugar transport, by physically interacting with the sucrose efflux transporter Sugar Will Eventually be Exported Transporter 11 (StSWEET11) to promote symplasmic sucrose transport (Abelenda *et al.*, 2019). While sugar transport is crucial for plant development throughout the life cycle, it plays a particularly important role during senescence, as it enables the mobilization of nutrients from senescing tissues to other parts of the plant for storage or further use (Wingler, 2018). A molecular link between both *StCDF1* and *StSP6A* with plant senescence has not yet been demonstrated.

To gain insight into how potato tuberization associates with leaf senescence, understanding the senescence regulatory network is important. The Arabidopsis NAC transcription factor ORESARA1 (ORE1) has been shown to act as a critical positive senescence regulator (Woo *et al.*, 2004; Rauf *et al.*, 2013; Qiu *et al.*, 2015; Kim *et al.*, 2018). ORE1 promotes senescence by directly binding to *BIFUNCTIONAL NUCLEASE1* (*BFN1*), *SENESCENCE-ASSOCIATED GENE 29* (*SAG29*) and other promoters of senescence-associated genes (Matallana-Ramirez *et al.*, 2013). *Arabidopsis thaliana AtORE1* mutants display a stay-green phenotype (Kim *et al.*, 2018). In the early development stages of plants, *AtORE1* is targeted and downregulated by the *miRNA164* at the transcription level (Kim *et al.*, 2009; Lira *et al.*, 2017). During leaf senescence, *miR164* expression is downregulated while *AtORE1* expression is enhanced (Pulido & Laufs, 2010). The balance between miR164 and AtORE1 transcripts is critical for leaf stage transition. Moreover, a number of *AtORE1* orthologues affecting leaf senescence and fruit quality traits have been identified in tomatoes, termed *SlORE1S02*, *3* and *6* according to their chromosomal position (Lira *et al.*, 2017).

Despite all previous research, knowledge about the regulation of senescence in potatoes is limited. In previous studies, *StCDF1* has been mapped as responsible for the onset of tuberization and senescence (Visker *et al.*, 2003; Kloosterman *et al.*, 2013; J. Li *et al.*, 2019). In this study, we present various facets of potato plant senescence, covering the onset and progression of senescence, as well as the assessment of the total life cycle length. *StCDF1* negatively affects the onset of senescence but accelerates the progression of senescence and shortens the life cycle. In addition, we identify the direct downstream target of *StCDF1*, *StORE1S02* (named by analogy to tomato), which has been found to regulate the onset of senescence specifically in potatoes. We also found that *StORE1s* play a key role in sugar transportation throughout several leaf developmental stages. This study discovered a new connection between tuber formation and senescence and provides insight into the molecular regulatory network of potato leaf senescence onset.

Materials and Methods

Plasmids and plant transformation

The sequences of *StCDF1.2*^{Coed} was synthesized by GenScript and cloned (Supporting Information Fig. S2, see later). Then, it was cloned into the pENTR™/D-TOPO vector (Invitrogen™; K240020) and then PK7GW2 by LR reaction (Invitrogen™; 11 791 020). The destination vector was transformed into the late tuberizing and senescence background potato CE3027 by Agrobacterium-mediated gene transformation (Visser *et al.*, 1989).

To knockdown all *StORE1s*, a 174 bp fragment targeted to all three *StORE1* genes was generated by using VIGS tool (https://vigs.solgenomics.net/). The fragment was cloned into pK7GWIWG2(II) to obtain the intron-spliced hairpin RNA(RNAi) construct and introduced into CE3130 (early senescence genotype) plants by Agrobacterium tumefaciens-mediated transformation. The full-length *StORE1S02* gene was cloned from CE3027 and inserted into the pK7GW2 vector. The plant transformation was done in the same process to CE3027 background.

Plant materials, growth conditions and sampling

In this experiment, two nontransgenic potato (*Solanum tuberosum* L.) lines were used: CE3130 and CE3027, which were offspring plants from the diploid C × E population (Celis-Gamboa, 2002; Ramírez Gonzales *et al.*, 2021). All plants were propagated in tissue culture by cutting.

Tissue culture plants (2 wk old) were transferred into 19 cm diameter pots filled with soil (102 060 Potting soil nr.4 Unifarm: 40 610 kg Horti Clay; 0.200 EN-m^3 MD Swedish sphagnum peat; 0.400 EN-m^3 Baltic peat medium; 0.400 EN-m^3 Garden peat Dolokal; 3820 kg Extra potting soil (bulk); 0.810 kg PG mix 15-10-20; pH: 5.70; EC: 0.80; EN factor: 1.23 HWW: 180) and grown in a controlled-environment chamber at LD condition (16 h : 8 h, light : dark, 22°C during the daytime and 18°C during the nighttime, at 70% relative humidity). The plants were regularly watered and received fertilizer (Osmocote) once at beginning (2 g per liter of soil). The pots were sorted into lines of 5. At least 10–20 cm distance was left in between lines to avoid shading.

Leaf samples for RNA isolation, chlorophyll isolation and sugar analysis were harvested from the mid part of source leaves

(fully expanded leaves, normally the 3–4th branch of leaves from the bottom, 1–2 cm up from leaf tip) at ZT3 (except the 24 h time course) and then frozen in liquid N_2, powdered and stored at −80°C.

Nicotiana benthamiana plants for transient assay were grown from seeds and were maintained in climate-controlled glasshouse compartments under a day and night regime of 22°C : 18°C, 16 h : 8 h, light : dark, at 70% relative humidity. The transient assays were preformed on the 4-5 wk old *Nicotiana benthamiana* plants.

RNA isolation and quantitative polymerase chain reaction

In order to quantify the relative expression levels of the targeted genes, RNA was isolated from fully expanded leaves using the MagMAX™ Plant RNA Isolation Kit (A33899) with the KingFisher™ Flex Purification System (5400610). One microgram of total RNA was reverse transcribed in 20 µl mixture with the iScript cDNA Synthesis Kit (Bio-Rad). The cDNA was diluted to a volume of 200 µl with MilliQ Water. Aliquots (2 µl) were then used as templates for subsequent real-time polymerase chain reaction (PCR) experiments. *StELF3e* was used as a housekeeping control (Kloosterman *et al.*, 2013; Ramírez Gonzales *et al.*, 2021), and primers of genes subjected to gene expression analysis are listed in Table S1. The relative gene expression levels were calculated using the delta CT method, normalized against *StELF3e* expression.

Statistical analysis of data

The statistical analysis was performed using Excel and GraphPad Prism 9. The specific statistical method was chosen based on data distribution and group comparison setup. The statistical method used is indicated in the legend.

Sugar content analysis

The leaf powder samples, each weighing 80 ± 2 mg, were supplemented with 500 µl of MilliQ water. The samples were then incubated at 80°C for 20 min with shaking. The tubes were centrifuged for 5 min at maximum speed and the supernatant was kept. 500 µl of MilliQ water was again added to the pellet and the steps were repeated 5 more times. To measure the sugar content, the Sucrose Assay Kit (Sigma-Aldrich; SCA20-1KT) was used. The absorbance was measured at 570 nm with TECAN infinite m plex plate reader.

Phylogenetic analysis

All sequences for phylogenetic analysis were retrieved from different database as follow: *Solanum tuberosum* L. (http://spuddb.uga.edu/), *Arabidopsis thaliana* L. (https://www.arabidopsis.org/), *Solanum lycopersicum* L. (https://solgenomics.net/), *Capsicum annuum* L. (https://solgenomics.net/), *Solanum melongena* L. (https://solgenomics.net/), *Lactuca sativa* L. (https://lgr.genomecenter.ucdavis.edu/), *Oryza sativa* L. (http://rice.uga.edu/), *Hordeum vulgare* L. (https://ics.hutton.ac.uk/barleyrtd/index.html), *Triticum aestivum* L. (https://academic.oup.com/plphys/article/180/3/1740/6117747#supplementary-data), *Brassica oleraceae* L., *Brassica rapa* L., *Brassica juncea* L., *Raphanus sativus* L. (http://brassicadb.cn/). The CDS were aligned by Muscle in the Dnastar Lasergene software. The phylogenetic tree was made in the software using the default settings.

Chlorophyll extraction and analysis

In Fig. 3(e) (see later), the total chlorophyll content was measured following the Lightenthaler (1987) protocol. First, the plant tissue was frozen, grinded, and weighed. Then, it was solubilized in 1 ml of 95% ethanol and heated at 80°C for 20 min. The solution was centrifuged for 5 min at 2800 G-force and the pellet was extracted. This step was repeated two more times with 1 ml ethanol 95%, and the amount of fresh biomass was calculated. All the supernatants were finally collected to constitute the extract. 200 µl of the extract was diluted in 1800 µl of 95% ethanol and measured at 648.6 and 664.2 nm using a spectrophotometer. Chl*a* and *b* were calculated using the following formulae (Guzzo *et al.*, 2021):

$$\text{Chl}a = 13.36 \times (\text{absorbance at } 664.2\,\text{nm}) - 5.19 \times (\text{absorbance at } 648.6\,\text{nm})$$

$$\text{Chl}b = 27.43 \times (\text{absorbance at } 648.6\,\text{nm}) - 8.12 \times (\text{absorbance at } 664.2\,\text{nm})$$

Chlorophyll measurement by chlorophyll meter

In Fig. 1(b), the chlorophyll content was measured using the Apogee MC-100 Chlorophyll Meter (https://www.apogeeinstruments.com/chlorophyll-meter-support/) at ZT3, following the manufacturer's guidelines and utilizing the generic settings. The sampling was done with the mid part of source leaves (fully expanded leaves, normally the 3–4th branch of leaves from the bottom, 1–2 cm up from leaf tip).

Chlorophyll fluorescence measurement

In Fig. 1(c), the parameters of chlorophyll fluorescence were measured by LI-600 porometer/fluorometer (https://www.licor.com/env/products/LI-600) at ZT3, following the manufacturer's guidelines. The sampling of leaf tissue was performed the same as in the chlorophyll measurement.

DAP-Seq Illumina library preparation and analysis

DNA Affinity Purification and sequencing (DAP-Seq) experiments was preformed by (Gonzales, 2022) with full described mythology. In brief, the gDNA (genomic DNA) from stolons of *S. tuberosum* group andigena plants was isolated using the CTAB method (Doyle, 1991) with three independent replicates. Further, the isolated gDNA was quantified with Qubit 4

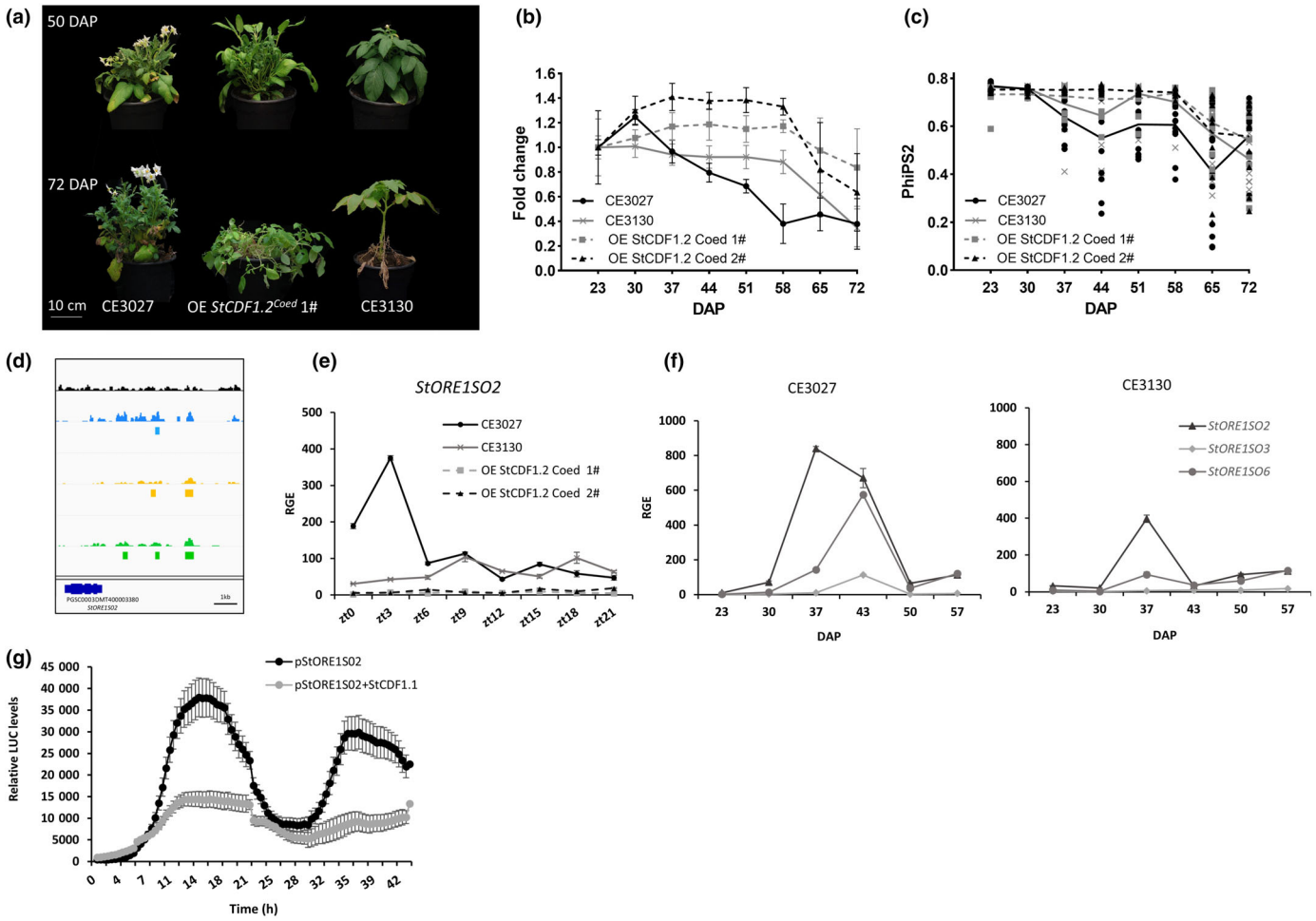

Fig. 1 StCDF1 repress expression of *StORE1S02* via directly binding to the promoter of *StORE1S02* in *Solanum tuberosum*. (a) Phenotype of CE3027 (long life cycle, late tuberizing, homozygous for *StCDF1.1*), CE3130 (short life cycle, early tuberizing, containing both the *StCDF1.2* and *StCDF1.3* alleles), OE *StCDF1.2*^{Coed} 1# at 50 and 79 days after planting (DAP). (b) Fold change of chlorophyll content (μmol of chlorophyll per m^2, measured by Apogee MC-100 Chlorophyll Meter) from 23 to 72 DAP in CE3027, CE3130, OE *StCDF1.2*^{Coed} 1# and OE *StCDF1.2*^{Coed} 2#. The chlorophyll content of each line was standardized to a value of 1 at 23 DAP. Error bars: means ± SE, with $n = 12$ technical replicates. (c) Quantum yield of PSII (in light, measured by Licor-600) of the same samples from (b). Each measurement was plotted as one data point, $n = 12$ technical replicates. The average of data points from the same time and plant line are connected by a line. (d) DAP-Seq (DNA affinity purification sequencing) binding peaks of StCDF1 in the promoter region of *StORE1S02*. Diagram description from the top: input library as negative control (black bar chart), experiment 1 (blue bar chart), experiment 2 (yellow bar chart), experiment 3 (green bar chart). The significant binding sites are shown as colored blocks below the bar charts of each experiment. The gene model of *StORE1S02* is represented in blue. In the right bottom corner, the scale represents 1 kb. (e) Diurnal gene expression analysis of *StORE1S02* in CE3027, CE3130 and OE *StCDF1.2*^{Coed} 1# and OE *StCDF1.2*^{Coed} 2#. RGE: relative gene expression. ZT, Zeitgeber time. Error bars: means ± SE, with $n = 3$ biological replicates. (f) Transcript profiles of *StORE1s* throughout development in CE3130 and CE3027. Error bars: means ± SE, with $n = 3$ biological replicates. (g) Repression of p*StORE1S02*::iLUC luciferase activity by 35S::*StCDF1.1* in *Nicotiana benthamiana* leaves. The p*StORE1S02* were used as a negative control. Relative luminescence units (RLU) was measured at intervals of 30 min for 40 h in total. Values are given as median ± SD, $n = 16$.

fluorometer and fragmented in a Covaris M220 Focused-ultrasonicator with target size 200 bp. DNA-ends were trimmed, A-overhangs created, and the adapters ligated. Adapters were generated by annealing the oligonucleotides Adapter A 5′-ACACTCTTTCCCTACACGACGCTCTTCCGATCT-3′ and Adapter B 5′-GATCGGAAGAGCACACGTCTGAACTC-CAGTCAC-3′.

The coding sequences of the *StCDF1.1* (used in experiment 1&2) and *StCDF1.2* (used in experiment 3) were fused to maltose-binding proteins (MBP) in pDEST-TH1 vector. Then, the recombined constructs transformed into *Escherichia coli* Rosetta cells to produce the recombinant proteins. Soluble extracts derived from induced *E. coli* cultures expressing MBP-CDF fusions were used to obtain recombinant proteins. Subsequently, 400 μl of clarified protein extracts were incubated with a potato gDNA library at a concentration of 400 ng. We utilized Amylose Magnetic Beads from New England Biolabs for the binding of MBP fusion proteins and the purification of protein-DNA complexes. Then, 20 cycles of PCR were performed using the recovered DNA with following primers: Primer A (Illumina TruSeq Universal_Primer) 5′AATGATACGGCGACCACCG AGATCTACACTCTTTCCCTACACGACGCTCTTCCGAT

CT 3′ and Primer B: Illumina TruSeq Index Primer:5′ CAAGCAGAAGACGGCATACGAGAT-NNNNNN-GTGAC TGGAGTTCAGACGTGTGCTCTTCCG 3′. For Primer B, NNNNNN is 'ATCACG', 'CGATGT' or 'ATCACG' for experiments 1, 2 and 3, respectively. As a negative control, we generated an input library by directly amplifying the gDNA library for 10 cycles. Subsequently, the DNA was further purified and quantified using the previously described methods. The indexed libraries underwent sequencing using Illumina HiSeqX (PE 2 × 50, experiment 1 and input sample) by Novogene (Cambridge Lab, Cambridge, UK), and MiSeq V3 (PE 2 × 75, experiments 2 and 3). The analysis of reads sequencing results is described in Gonzales (2022).

Transient dual-luciferase reporter system

The putative promoter regions for *StORE1S02* and *StSWEET11* were amplified from CE3027 using primers designed based on the DM1-3-56-R44 v4.04 genome sequence, as specified in Table S1. The *StORE1S02* promoter region was set as the region up to 4 kb upstream of the transcription start site which included the sequence bound by StCDF1 obtained from the DAP-Seq analysis (Fig. 1d). The StSWEET11 promoter was set as the region up to 3 kb upstream of the transcription start site (Fig. S4A, see later). The PCR amplification products of both promoters were cloned into GATEWAY cloning vector pDONR221 or pDONR207 and later inserted into pGWB435-iLUC destination by LR Clonase reaction (Invitrogen).

The *StORE1S02mDAP* promoter sequence was modified from the 4.0 kb *StORE1S02* promoter fragment previously cloned into pDONR207. This mutagenesis aimed to modify the second 250 bp proximal peak region, identified in experiments 2 and 3 of the StCDF1 DAP sequencing results (Gonzales, 2022). Primers were designed flanking the CDF1 binding DAP-seq peak region, introducing a *Bam*HI restriction enzyme site. Subsequently, the PCR product underwent *Bam*HI digestion to create sticky ends. The digested PCR product was then subjected to ligation using T4 DNA ligase (Promega). The resulting ligation mixture was subsequently transformed into a DH5α strain of *E. coli*. Identification of constructs containing the desired mutation was achieved through restriction digestion. Finally, validation of the mutations was carried out through DNA sequencing, before cloning it into the pGWB435iLUC destination vector.

These reporter constructs were transformed in *Agrobacterium tumefaciens* strain (AGL1) and co-infiltrated into *Nicotiana benthamiana* (rdr6i) leaves with 35S::*StCDF1.1* (full length) constructs. Agrobacterium strains resuspended in MMAi buffer (10 mM MES (pH 5.8), 10 mM MgSO4 and 150 μM acetosyringone). A final concentration of 0.2 OD_{600} for all constructs was used for infiltration. Two days' postinfiltration leaf disks were incubated in 2 × MS plant medium supplemented with 0.02 mg ml^{-1} D-luciferin (Promega). Luciferase activity was recorded every 30 min in Centro LB-960 microplate luminometer (Berthold Technologies, Bad Wildbad, Germany), using MIKROWIN 2000 (v.4.29) software.

Results

StCDF1 represses senescence onset and shortens growing period

Previously, we showed that overexpressing a truncated *StCDF1* (*StCDF1.2*) in a late tuberizing background (homozygous *StCDF1.1*), not only induced early tuberization but also shortened life cycle length (Kloosterman *et al.*, 2013; Hoopes *et al.*, 2022). By contrast, knocking down *StCDF1* in an early tuberizing background (heterozygous StCDF1.2/1,3) resulted in extended life cycle length (Fig. S1). To study the function of *StCDF1* in regulating senescence, we selected two offspring plants of the C × E population described previously (Kloosterman *et al.*, 2013; Ramírez Gonzales *et al.*, 2021) with different *StCDF1* allele combinations for observing senescence-related traits in detail (Fig. 1a). To study the impact of StCDF1 in regulating senescence, we aimed at overexpressing StCDF1 in a late background. Due to the better protein stability, StCDF1.2 was selected as backbone (Kloosterman *et al.*, 2013). Furthermore, to avoid negative regulation by the lncRNA *StFLORE* transcript (Ramírez Gonzales *et al.*, 2021) and thereby ensuring high expression throughout the day, we edited the coding usage in the 35S:*StCDF1.2* construct (Fig. S2) resulting in a construct named p35S:$StCDF1.2^{Coed}$. Strong expression of p35S:$StCDF1.2^{Coed}$ was found in transgenic lines (Fig. S3).

Interestingly, although a longer life cycle was observed in CE3027 (homozygous *StCDF1.1*), the lowest leaves have visible yellowing (50 DAP) earlier than those in CE3130 (early tuberizing, containing two truncated *StCDF1* variants: the *StCDF1.2* and *StCDF1.3* alleles) and OE $StCDF1.2^{Coed}$ (Fig. 1a). The visible leaf yellowing in CE3130 started at 72 DAP and it rapidly completed its life cycle within 1 wk. The weekly measurements of chlorophyll content consistently demonstrate a gradual decline in the lower leaves of CE3027 starting from 37 DAP. By contrast, the chlorophyll content in OE $StCDF1.2^{Coed}$ and CE3130 plants appears to remain relatively stable until reaching 65 DAP (Fig. 1b). We observed a similar pattern in change of chlorophyll fluorescence (quantum yield of PSII) through the time (Fig. 1c). Together, the delayed senescence onset and shortened life cycle also were clearly visible in overexpressing $StCDF1.2^{Coed}$ transgenics (Fig. 1a–c).

These phenotypes suggest that senescence-related traits, like senescence onset, speed of senescence progression and life cycle length are not positively correlated in potato. Overexpressing $StCDF1.2^{Coed}$ in a late background or carrying a truncated *StCDF1* allele (*StCDF1.2/1.3*) will shorten the life cycle, but delay senescence onset. In summary, *StCDF1* repress senescence onset and reduced life cycle length.

StCDF1 binds to and represses the expression of a positive senescence regulator, *StORE1S02*

To understand how *StCDF1* is involved in the regulation of senescence, this study used the direct target genes of StCDF1. Recently, a DAP-seq (DNA Affinity Purification and sequencing)

of StCDF1 was performed by Gonzales (2022) and this dataset revealed many novel direct downstream targets of StCDF1. By manually screening for well-known senescence regulators, we found that there are multiple binding sites for StCDF1 on the promoter of *StORE1S02* (*StORESARA1S02*; Fig. 1d), whose orthologues positively regulate senescence in Arabidopsis and tomato (Lira *et al.*, 2017). Based on the DAP-seq results, we hypothesized that *StCDF1* might directly regulate the expression of *StORE1S02*. Therefore, we examined the expression of *StORE1S02* in CE3130 and OE *StCDF1.2*^{Coed} transgenics and the background of these transgenics (CE3027). The results show that during the early light period (ZT0-ZT3), transcription levels of *StORE1S02* in CE3130 and OE *StCDF1.2*^{Coed} transgenics were strongly downregulated compared to CE3027 (Fig. 1e; Table S2).

This repression can also be found in the *StORE1S02* expression profile during the development (23-57DAP; Fig. 1f) in CE3130 compared to CE3027. Although the *StORE1S02* transcript level reached its highest point at 37 DAP in both early and late backgrounds, the upregulated period of *StORE1S02* is longer in CE3027 (30 DAP-50 DAP) than in CE3130 (30 DAP-43 DAP). To further confirm that the reduced expression of *StORE1S02* is linked to the repressing function of *StCDF1*, the 35S:*StCDF1.1* construct was co-infiltrated into tobacco leaves with *StORE1S02* promoter constructs driving expression of the firefly luciferase gene (Fig. 1g). The result shows that StCDF1 downregulates the expression of *StORE1S02*. Moreover, by mutating one predicted StCDF1 binding sites, the repression effect is reduced by over 35% (Fig. S4). Together, StCDF1 binding to the promoter of *StORE1S02* and the co-expression study confirms that StCDF1 directly negatively regulates the expression of *StORE1S02*.

ORE1 orthologs in potato

ORESARA1 (*ORE1*) encodes a NAC transcription factor that positively regulates senescence by promoting nucleic acid degradation and inhibiting chloroplast maintenance (Matallana-Ramirez *et al.*, 2013; Rauf *et al.*, 2013). In this study, we identified 3 ORE1 orthologs in potato by comparing protein sequences from *Arabidopsis thaliana* and *Solanum lycopersicum* (*AtORE1*, *SlORE1S02*, *SlORE1S03*, and *SlORE1S06*) against the potato reference genome DM 1–3516 R44 v6.1. The identified homologs were named *StORE1S02*, *StORE1S03* and *StORE1S06* according to their chromosome localization, as with the tomato *SlORE1* genes. The coding sequence (CDS) of the genes were aligned and a phylogenetic representation including all *ORE1* sequences from the different crops was created (Fig. 2a). Interestingly, unlike other plant families, all analyzed Solanaceae species had 3 copies of *ORE1*.

By retrieving and analyzing the CDS of *ORE1* from 13 species, we found that all Solanaceae species carry an in-frame insertion of 24 bp in the *ORE1S02* homolog (Fig. 2b). This insertion was suggested to disrupt the binding and the cleaving by *miR164* (Lira *et al.*, 2017). We performed a diurnal gene expression analysis of *StORE1* genes in the diploid potato genotype CE3027 and show that *StORE1S02* has a much higher expression than the other two at four different time points (ZT0, ZT3, ZT6 and ZT12; Fig. 2c). The same pattern can also be found over the development period (Fig. 1f). Therefore, the transcript abundance of *StORE1S02* is the highest among all three ORE1 orthologs in potato.

StORE1S02 positively regulates senescence onset

Based on phylogenetic analysis and diurnal gene expression analysis, *StORE1S02* is the closest ortholog to *AtORE1* and has the highest expression among all three *StORE1* genes (Fig. 2a,c). Therefore, for the p35S:*StORE1S02*, 3 transgenic lines were generated in the long life cycle diploid potato genotype CE3027. The results show both selected transgenic lines (OE#11, OE #21) displayed higher expression of *StORE1S02* (Fig. S5) and they all showed an early senescence phenotype (Fig. 3a). However, overexpressing *StORE1S02* did not shorten the life cycle compared to the background CE3027 (Fig. 3b).

Interestingly, in both overexpressing *StORE1S02* transgenic lines the expression levels of *StORE1SO3* and *StORE1SO6* were upregulated. This result suggests *StORE1S02* may positively regulate *StORE1SO3* and *StORE1SO6* expression (Fig. 3c).

To further confirm the function of *StORE1s* in potato and avoid possible redundant effects of different homologs, we selected the region which is highly similar among all three *StORE1s* as RNAi targeting region (Fig. S6). *StORE1s* knockdown plants were generated in CE3130, a short life cycle background. Two lines (KD#3 and KD #4) were selected for use in this experiment. A delayed senescence phenotype was found in the *StORE1s* knockdown lines (Fig. 3d). The chlorophyll level also indicates that these transgenic lines contain less chlorophyll a and b compared with the background genotype (Fig. 3e). The life cycle length of KD lines is extended for an extra 3 wk, but their life cycle still ended earlier than CE3027 and both OE lines (Fig. 3f).

BIFUNCTIONAL NUCLEASE1 (*BFN1*) has been reported to be positively regulated by *ORE1* in *Arabidopsis* (Matallana-Ramirez *et al.*, 2013). In our transgenic lines, we found that *StBFN1* expression was significantly downregulated in KD#3 and KD#4 lines and upregulated in OE#11 and OE#21 lines, compared to their background plants separately (CE3130 and CE3027; Fig. 3g). Thus, we confirmed that this senescence-associated gene *StBFN1* is positively regulated by StORE1 transcription factors. By checking the senescence phenotype and senescence-related gene expression of both OE and KD lines, we provide strong evidence that StORE1 proteins act as positive regulator for senescence, especially the senescence onset timing, in potato.

StORE1 genes do not affect tuberization initiation but affect sugar transportation

To address whether *StORE1S02* genes have an impact on tuberization, the tuberization phenotype was examined in the *StORE1*-RNAi lines and their background plants (CE3130) at 35 DAP.

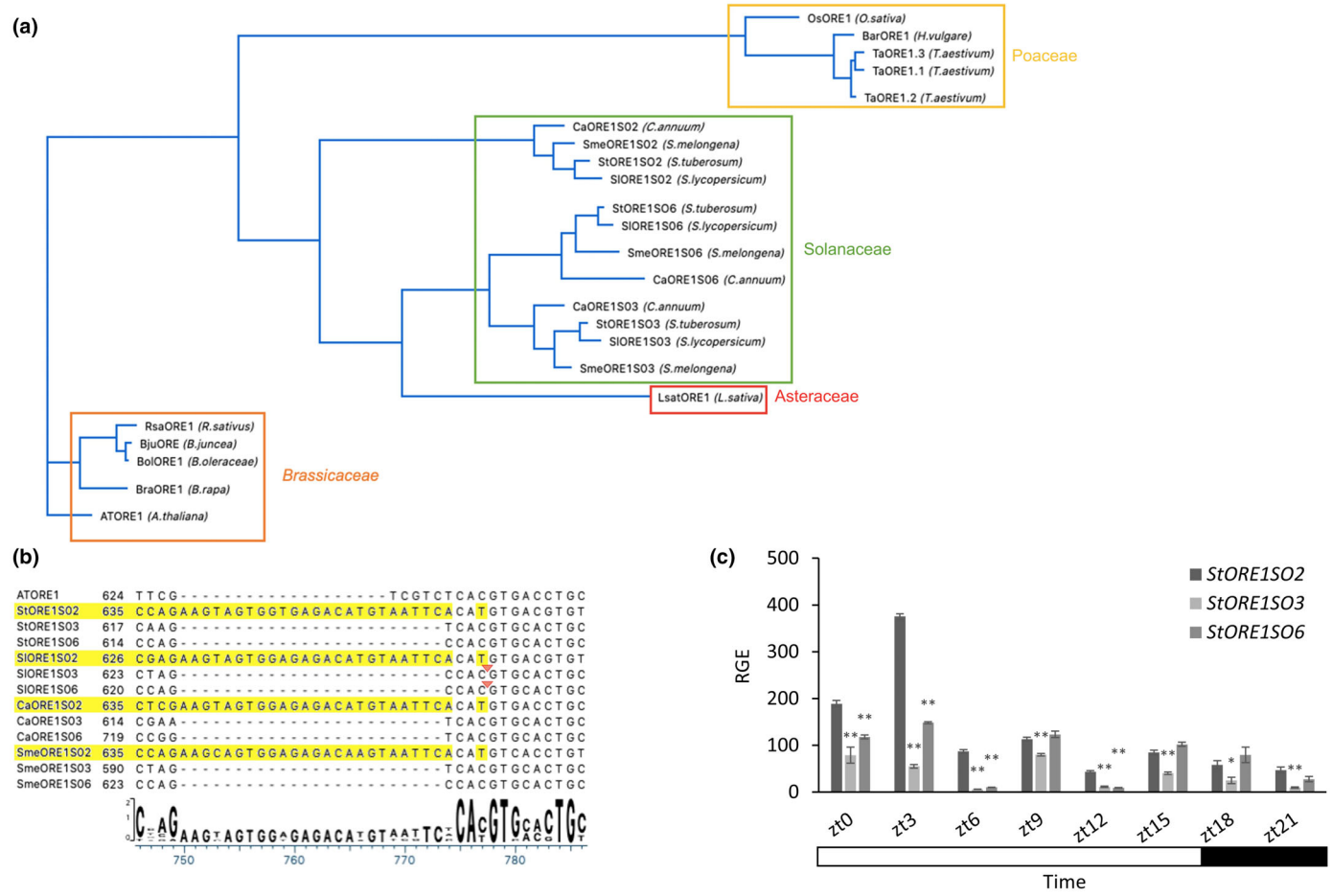

Fig. 2 *ORE1* orthologs in *Solanum tuberosum*. (a) Phylogenetic representation of the *ORE1* genes obtained from the alignment of their protein sequences. The different species are clustered by family. Three *AtORE1* orthologs were found for all Solanaceae species. All sequences are detailed in Supporting Information Table S3. In potato, they were named as follows: *StORE1S02*, *StORE1S03*, and *StORE1S06*. (b) Alignment of *AtORE1* and its orthologs in four Solanaceae species. The miRNA164 binding site in *ORE1S02* genes is highlighted in yellow. The red arrowheads correspond to the *SlmiRNA164* cleavage sites detected by Lira *et al*. (2017), in *StORE1S03* and *StORE1S06*. (c) Analysis of *StORE1* gene expression in CE3027 across the diel. Error bars: means ± SE, with $n = 3$ biological replicates. *, $P < 0.05$; **, $P < 0.01$; Compared to *StORE1S02*; *t*-test.

In previous experiments, CE3130 started tuberizing *c.* 30–35 DAP. Both KD lines produced tubers at 35 DAP, as did CE3130 (Fig. 4a). In order to confirm the molecular state underlying the tuberization phenotype, the expression of *StSP6A* in the transgenic lines was measured (Fig. S7). The *StSP6A* expression remained high in these KD lines. These results demonstrate that StORE1 proteins do not function as a trigger of tuberization.

During the observation period, leaf thickening was found in KD lines (Fig. 4b). We speculated that leaf thickening and cell enlargement could be an indication of increased sugar accumulation. To test our hypothesis, we analyzed the sucrose and glucose content in the leaves at 4 different time points. In the KD lines, the sucrose content increased through time. By contrast, the sucrose content in CE3130 plants remained the same between these 4 time points (Fig. 4c). The glucose content remained relatively stable in all plant lines through these 4 different time points (Fig. S8). We further checked the chlorophyll fluorescence and there was no significant difference between KD plants and their background plants (CE3130) among all the time points (Fig. 4e). Together, we observed that under the same photosynthesis rate, sucrose accumulated in the leaves of *StORE1s* knockdown plants throughout the development, but not in their background plant (CE3130).

Senescence-associated genes (*SAGs*) are a group of genes that have been found to be upregulated during senescence in various species (Lohman *et al*., 1994; Gepstein *et al*., 2003). SAGs are, therefore, used as molecular markers for detecting senescence (Gepstein *et al*., 2003; Zhang *et al*., 2021). *SAG29* has been found to be a direct transcriptional target of *ORE1* in *Arabidopsis* (Matallana-Ramirez *et al*., 2013) and the induced expression of *SAG29* has been found to be associated with leaf yellowing (Kamranfar *et al*., 2018). Interestingly, SAG29 is also known as a member of the clade III SWEET proteins (*SWEET15*). We show that the expression of *StSAG29* was strongly repressed throughout different developmental stages (37DAP and 43DAP) in RNAi *StORE1S02* lines compared with CE3130 (Fig. 4d). This is consistent with an increased sucrose content found in the leaves (Fig. 4c). By contrast, *StSAG29* has a higher expression in OE

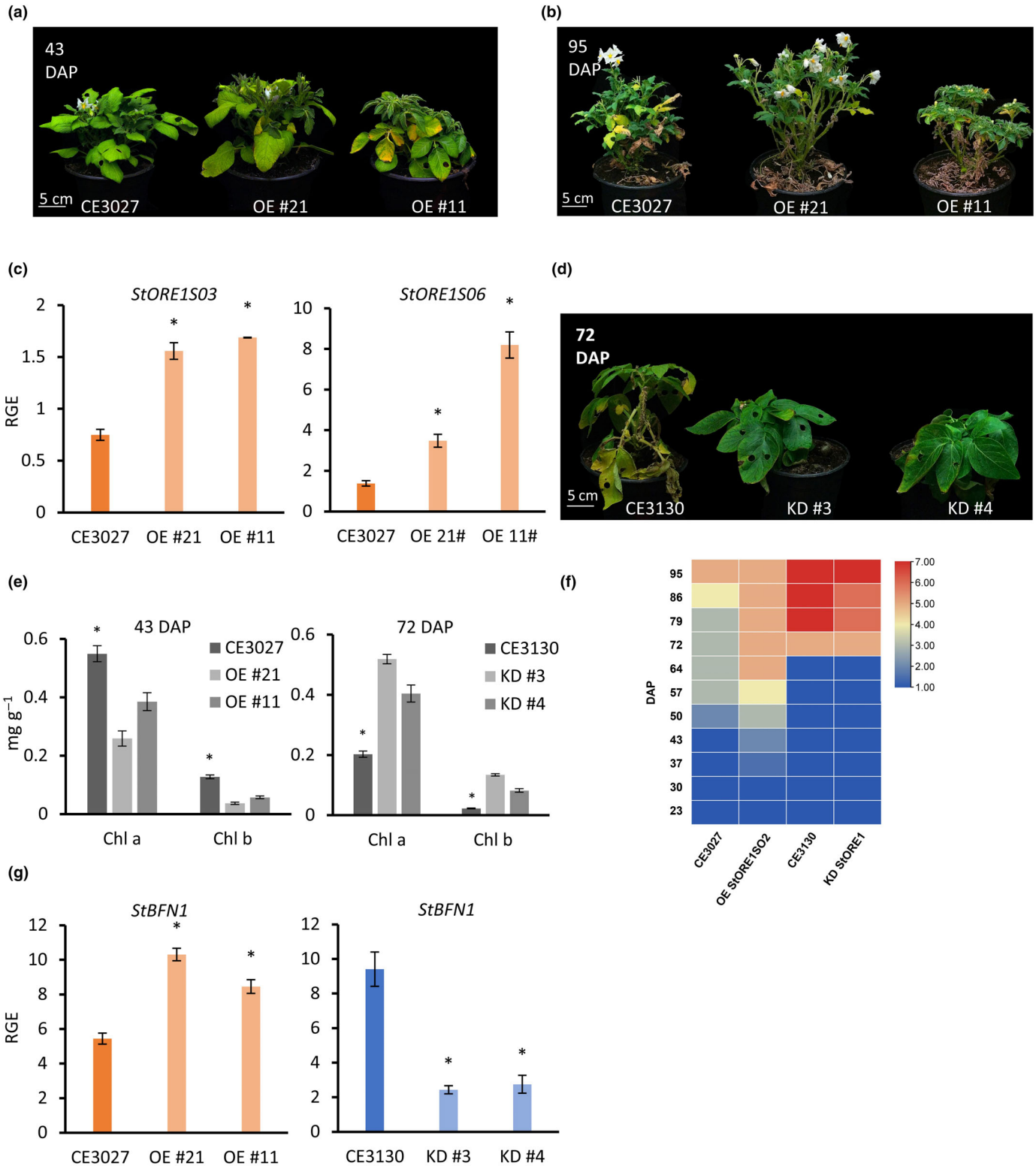

lines than in CE3027 (Fig. S9). Besides *StSAG29/SWEET15*, the expression of *StSWEET11* was also found to be increased in both *StORE1S02* overexpressed lines and decreased in both *StORE1* knockdown lines (Fig. 4f). To further confirm this regulation, we performed a transient assay. The *35S::StORE1S02* construct was co-infiltrated into tobacco leaves with *StSWEET11* promoter construct driving expression of the firefly luciferase gene. The results show StORE1S02 can activate expression of *StSWEET11* (Fig. S10). We also investigated the expression of *StHXK1*, a well-known player in sugar signaling that regulates leaf

Fig. 3 *StORE1S02* positively regulates senescence. (a) From left to right, CE3027 and CE3027 transformed with 35S::*StORE1S02* lines 21 and 11 (OE #21 and OE #11) at 43 days after planting (DAP). (b) From left to right, CE3027 and CE3027 transformed with 35S::*StORE1S02* lines 21 and 11 (OE #21 and OE #11), at 95 DAP. (c) Relative expression of *StORE1SO3* and *StORE1SO6* in CE3027 and CE3027 transformed with 35S::*StORE1S02* lines 21 and 11 (OE #21 and OE #11) at 23 DAP. Data are presented as the mean ± SE biological triplicates. *, $P < 0.05$; *t*-test. (d) From left to right, CE3130 and *StORE1S02* knockdown lines in the CE3130 background (KD #3 and KD #4) at 72 DAP. (e) Analysis of chlorophyll content in CE3027, OE #21 and OE #11 at 43 DAP. And chlorophyll content in CE3130, KD #3 and KD #4 at 72 DAP. Data are presented as the mean ± SE biological triplicates. *, $P < 0.05$; *t*-test. Samples from each line were pooled (5 individuals) and measured. (f) Heat map shows the senescence development. Senescence scoring according to the instructions from Hurtado *et al*. (2011), with minor modifications: 1 = green plant; 2 = upper leaves with the first signs of yellowing (light green); 3 = yellow leaves; 4 = 25% of canopy brown; 5 = 50% of canopy brown; 6 = > 75% canopy brown; 7 = dead plant. (g) Relative expression of *StBFN1*. The gene expression results of CE3130 and *StORE1S02* knockdown lines in CE3130 background (KD #3 and KD #4) at 37 DAP are shown in blue. The gene expression results of CE3027 and CE3027 transformed with 35S::*StORE1S02* lines 21 and 11 (OE #21 and OE #11) at 23 DAP are shown in orange. Data are presented as the mean ± SE biological triplicates. *, $P < 0.05$; *t*-test.

senescence (Moore *et al*., 2003). However, no significant difference was found between the KD lines and CE3130 (Fig. S11). These results indicate that *StSWEET11* and *SAG29/SWEET15* expression are associated with senescence and regulated by the StORE1 transcription factors.

Compared to the extended life cycle of KD plants, the CE3130 plants finished their life cycle 3 wk earlier. We harvested all CE3130 and half of the KD plants and measured total tuber weight at 72 DAP. The other half of the KD plants was harvested at 95 DAP. In the first harvest, the total tuber weight of CE3130 was higher than all KD lines (Fig. 4g). In the second harvest, both KD lines achieved higher yield compared to the first harvest. However, the total yield of KD lines in the second harvest showed no significant difference to the total yield of CE3130 (Fig. 4g).

We also compared the total yield from *StORE1S02* overexpressing lines with their background CE3027. The yield of both OE #11 and OE #21 plants was significantly reduced compared to the background (CE3027; Fig. 4h). Among these transgenics, the higher expression of *StORE1S02*, the greater the reduction in yield. The OE #11 line, which has the highest expression of *StORE1S02* (Fig. S5), failed to make any tubers. The OE #21 line has a lower expression level of *StORE1S02* compared to line #11 and is able to make tubers but the yield is significantly reduced (Fig. 4h).

These results together indicate that knocking down *StORE1S02* expression may delay the sugar transport from leaf to tuber but has no significant impact on yield in practice. However, overexpressing *StORE1S02* significantly reduced the yield. Thus, *StORE1s* play a key role in sugar transportation and premature senescence caused by overexpressing *StORE1S02* will lead to severe yield loss.

Discussion

Potato aboveground maturity is considered to be an important trait for potato production, especially regarding the final yield. In many other plants such as wheat, tomato, delayed senescence contributes to longer periods of photosynthesis and can increase final yield (Lira *et al*., 2017; Joshi *et al*., 2019). However, in potato, previous field studies indicated this link between senescence and final yield is more complicated. Clot *et al*. (2023) reported that the C x E population showed a negative correlation between life cycle length and yield, and we observed the same in the genotype CE3027 in this research. By contrast, a positive correlation between long life cycle and high yield is seen in commercial potato breeding programs (Stöckle *et al*., 2010; Kleinwechter *et al*., 2016; Yuan *et al*., 2016). The varieties used in these breeding programs have undergone selection for early tuberization and late senescence in order to achieve high yield and high starch content (Hoopes *et al*., 2022; Clot *et al*., 2023). Therefore, the genotypes from research populations that have not undergone this selection, could consequently show a different correlation. Consequently, using research populations with a wider genetic base could help uncover the biological functions underlying the correlations between life cycle length and yield.

Allelic variation of *StCDF1* has been found to influence various developmental traits including tuberization, senescence and yield (Kloosterman *et al*., 2013). Having a truncated *StCDF1* (*StCDF1.2/1.3*) not only promotes early tuberization and shortens life cycle length but also has major impact on yield (Kloosterman *et al*., 2013; Manrique-Carpintero *et al*., 2015; Marand *et al*., 2019; Hoopes *et al*., 2022; Clot *et al*., 2023). Thus, it is apparent that StCDF1 plays a complex role in regulating potato plant development.

In this study, we demonstrated that *StCDF1.2* has different effects on three senescence-related traits. Our data indicate that plant senescence is not a single quantitative trait, but a combination of several morphological traits including senescence onset, senescence progression speed and total life cycle length. Constitutive overexpression of *StCDF1* delays senescence onset but promotes more rapid senescence progression and shortened life cycle length (Fig. 1a). This result indicates that these senescence-related traits are not associated with each other but regulated separately.

We identified a direct downstream target of *StCDF1*, which has been known to act as a positive senescence regulator in other crops, *StORE1S02* (Woo *et al*., 2004; Lira *et al*., 2017). In potato (*Solanum tuberosum*), three *ORESARA1* homologs are present; *StORE1S02*, *StORE1S03*, and *StORE1S06*. Among these three homologs, *StORE1S02* is the closest to *SlORE1S02* and shares the feature of an insertion near the binding sites of the *miRNA164* (Lira *et al*., 2017). This is the case also for eggplant (*S. melongena*) and Capsicum (*C. annuum*), which also belong to the Solanaceae family of plants.

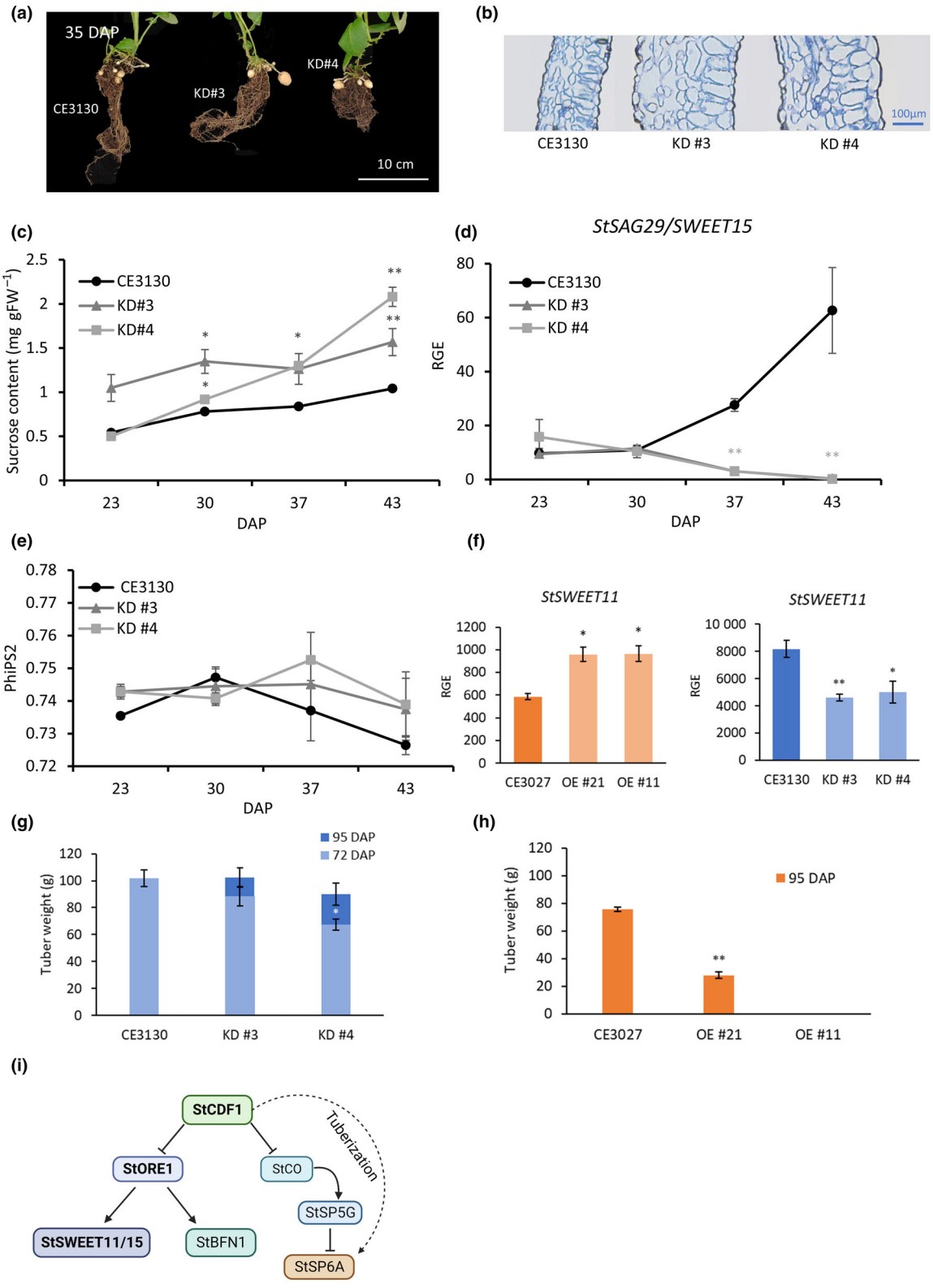

In this study, we confirmed that *StORE1S02* acts as a positive regulator for leaf senescence in potato, as has been seen in other plant species (Rauf *et al.*, 2013; Lira *et al.*, 2017), specifically regulating senescence onset. Overexpressing *StORE1S02* in CE3027, which has a late tuberization time and a long life cycle, induced early yellowing in the lower leaves, but life cycle length was not affected. In the young/top leaves, overexpressing *StORE1S02* interestingly failed to induce cell death and leaf

Fig. 4 *StORE1S02* affects sugar transport in *Solanum tuberosum*. (a) From left to right, underground phenotype of CE3130 and *StORE1S02* knockdown lines in CE3130 background (KD #3 and KD #4) at 35 days after planting (DAP). (b) Light microscopy image of a leaf cross section of CE3130 and *StORE1S02* knockdown lines (KD #3 and KD #4). The leaves were harvested at 30 DAP. (c) Sucrose content in leaves of CE3130 and *StORE1S02* knockdown lines in CE3130 background (KD #3 and KD #4) at different time points (23, 30, 37 and 43 DAP). (d) Relative expression of *StSAG29/SWEET15* in CE3130 background (KD #3 and KD #4) at different time points (23, 30, 37 and 43 DAP). Data are presented as the mean ± SE biological triplicates. **, $P < 0.01$; *t*-test. (e) Quantum yield of PSII (in light, measured by Licor-600) of CE3130 and *StORE1* knockdown lines in CE3130 background (KD #3 and KD #4) at different time points (23, 30, 37 and 43 DAP). Error bars represent the SE of the mean. (f) Relative expression of *StSWEET11*. The gene expression results of CE3130 and *StORE1S02* knockdown lines in CE3130 background (KD #3 and KD #4) at 37 DAP are shown in blue. The gene expression results of CE3027 and CE3027 transformed with 35S::*StORE1S02* lines 21 and 11 (OE #21 and OE #11) at 23 DAP are shown in orange. Data are presented as the mean ± SE biological triplicates. *, $P < 0.05$; **, $P < 0.01$; *t*-test. (g) Average of tuber weight per plant for knockdown plants and their background CE3130. *, $P < 0.05$; **, $P < 0.01$; *t*-test. Error bars represent the SE of the mean. (h) Average of tuber weight per plant for overexpressed plants and their background CE3027. *, $P < 0.05$; **, $P < 0.01$; *t*-test. Error bars represent the SE of the mean. (i) A hypothetical model for the function of StCDF1 in regulating tuberization and senescence suggesting that StCDF1 represses the expression of *StCO* and *StSP5G*, indirectly promoting *StSP6A* expression to facilitate tuberization. Simultaneously, StCDF1 negatively regulates *StORE1S02* at the transcriptional level. StORE1S02, when activated, promotes leaf senescence by enhancing the expression of genes involved in nucleic acid degradation (*StBFN1*) and sugar transportation processes (*StSWEET11&15*).

yellowing. We hypothesize that either the *StORE1S02* transcript or its protein's function was blocked in the young/top tissue. Other than posttranscriptional regulation by *miRNA164*, a kinase-based posttranslational mechanism was reported by Durian *et al.* (2020). Furthermore, the ORE1 protein undergoes ubiquitin-mediated degradation, which is influenced by the nitrate state (Park *et al.*, 2018). Therefore, we propose that the lack of impact on the top/young leaves when overexpressing *StORE1S02* may be attributed to distinct posttranslational modifications within various tissues, such as phosphorylation and polyubiquitination. Altogether, we propose that the onset of plant senescence is regulated separately from the life cycle length of the whole potato plant and more experimentation is required to fully understand the molecular mechanism.

Previous studies in other crops reported that early leaf senescence has a large negative impact on final yield (Xujun *et al.*, 2005; Ma *et al.*, 2018; Yang *et al.*, 2020). In this study, we demonstrate the reduction in final yield, by inducing early senescence in potatoes. In addition, we found that the lower fully expanded leaves play an essential role as source leaves for tuberization and final yield accumulation, while the upper sink leaves do not. This result provides insight into the interesting negative correlation between long life cycle length and low yield in potato genotypes like CE3027. This genotype has a long life cycle due to apical meristem maintenance keeping young top leaves green. However, the photosynthesis in these top young leaves does not contribute to final yield. Considering yield is a highly polygenic trait, it is possible that senescence onset and senescence progression speed were already inadvertently selected for during breeding for high yield in the past. In most of these breeding programs, senescence was treated as an individual trait, phenotyped at a single time point. Our research provides the novel insight that the different senescence components can all influence final yield. This allows for more precise selection of traits in breeding. For example, for late maturing genotypes which already have a long life cycle, targeted selection for delaying senescence onset or slowing down the senescence progression might be the route to improve the final yield.

The increased sucrose content in leaves and reduced expression of *StSWEET11&15*, together with the delayed tuber growth, suggest sugar transport from leaves to tuber was negatively regulated in KD lines. Sugar signaling has a significant impact on leaf senescence (Hoeberichts *et al.*, 2007; van Doorn, 2008; W. Li *et al.*, 2019). However, whether leaf senescence is promoted by sugar accumulation or by sugar deficiency is still remains unresolved (Pourtau *et al.*, 2006; van Doorn, 2008; Horacio & Martinez-Noel, 2013; Zhaowei *et al.*, 2020; Asim *et al.*, 2022). Here, we found that plants with low *StORE1S02* transcript display enhanced sugar accumulation in leaves and delayed leaf yellowing. This suggests that internal sugar accumulation is not the decisive factor for promoting early leaf senescence. Furthermore, our work provides a new mechanism for *ORESARA1* in inducing senescence, namely that StORE1s activate the expression of downstream sucrose efflux transporters to promote efficient phloem loading by SUC/SUT transporters. As such, we provide new evidence that leaf senescence contributes to tuber formation through nutrient release and rearrangement. Together, we propose that StORE1 transcription factors induce leaf senescence that contributes to tuber formation, especially as a stimulator for tuber bulking, but not as a tuberization inducer.

In potato, *StCDF1* regulates day-length-dependent tuberization onset by indirectly inducing the expression of *StSP6A* (Kloosterman *et al.*, 2013). StSP6A interacts with StSWEET11 to block sucrose leakage, promoting symplasmic transport of sucrose and tuber formation (Abelenda *et al.*, 2019). The fine balance between *StSP6A* and *StSWEET11* in expression level has a great impact on final yield (Abelenda *et al.*, 2019). In this study, we uncovered that StCDF1 represses senescence onset by directly repressing the expression of *StORE1S02*. StORE1S02, as an activator of *StSWEET* genes, bridges the gap between *StCDF1* and *StSWEETs*. Therefore, in the photoperiod-dependent tuberization regulation, StCDF1 promotes tuberization onset by keeping the expression balance of *StSP6A* and *StSWEETs* (Fig. 4i).

This new study sheds light on the mechanisms underlying potato development and yield potential, with important implications for potato breeding, particularly hybrid breeding. Our findings highlight the significant impact of *StCDF1* on regulating potato plant development and reproductive progress. To uncover additional genetic loci that regulate development, StCDF1 allelic variation should be considered in future breeding programs and incorporated into population designs.

Acknowledgements

We acknowledge the Wageningen University, Unifarm glasshouse and Klima employees for their help with the maintenance of the plants. We also thanking. Dirk-Jan Huigen for expert assistance in the glasshouse and growth-room trials. LS is supported by China Scholarship Council (No. 201807720077).

Competing interests

None declared.

Author contributions

LS and CWBB designed the research. LS and LdB performed a large part of the experiments and analyzed the data. MAS cloned the promoters and carried out the Transient transactivation assays. LS drafted the manuscript. LS, CWBB, MEdV, SUM, MAS and SP revised the manuscript. RGFV helped with overall supervision and critically edited the article. All authors read and approved the final manuscript.

ORCID

Christian W. B. Bachem https://orcid.org/0000-0002-3077-6833
Sybille Ursula Mittmann https://orcid.org/0000-0001-6168-2429
Salome Prat https://orcid.org/0000-0003-2684-5485
Maroof Ahmed Shaikh https://orcid.org/0000-0003-1512-2716
Li Shi https://orcid.org/0009-0008-4468-9360
Richard G. F. Visser https://orcid.org/0000-0002-0213-4016
Michiel E. de Vries https://orcid.org/0000-0002-1453-7672

Data availability

The full Dap-seq data set is described by Gonzales (2022). The rest study data are included in the article or the Supporting Information.

References

Abelenda JA, Bergonzi S, Oortwijn M, Sonnewald S, Du M, Visser RG, Sonnewald U, Bachem CW. 2019. Source-sink regulation is mediated by interaction of an FT homolog with a SWEET protein in potato. *Current Biology* **29**: 1178–1186.

Asim M, Zhang Y, Sun Y, Guo M, Khan R, Wang XL, Hussain Q, Shi Y. 2022. Leaf senescence attributes: the novel and emerging role of sugars as signaling molecules and the overlap of sugars and hormones signaling nodes. *Critical Reviews in Biotechnology* **43**: 1–19.

Celis-Gamboa BC. 2002. *The life cycle of the potato (Solanum tuberosum L.): from crop physiology to genetics*. PhD thesis, Wageningen University and Research, Wageningen, the Netherlands.

Clot CR, Wang X, Koopman J, Navarro AT, Bucher J, Visser RG, Finkers R, van Eck HJ. 2023. High-density linkage map constructed from a skim sequenced diploid potato population reveals transmission distortion and QTLs for tuber yield and pollen shed. *Potato Research*: 1–25. doi: 10.1007/s11540-023-09627-7.

van Doorn WG. 2008. Is the onset of senescence in leaf cells of intact plants due to low or high sugar levels? *Journal of Experimental Botany* **59**: 1963–1972.

Doyle J. 1991. DNA protocols for plants. In: Hewitt GM, Johnston AWB, Young JPW, eds. *Molecular techniques in taxonomy*. Berlin, Heidelberg, Germany: Springer Berlin Heidelberg, 283–293.

Durian G, Sedaghatmehr M, Matallana-Ramirez LP, Schilling SM, Schaepe S, Guerra T, Herde M, Witte C-P, Mueller-Roeber B, Schulze WX. 2020. Calcium-dependent protein kinase CPK1 controls cell death by *in vivo* phosphorylation of senescence master regulator ORE1. *Plant Cell* **32**: 1610–1625.

Gepstein S, Sabehi G, Carp M-J, Hajouj T, Nesher MFO, Yariv I, Dor C, Bassani M. 2003. Large-scale identification of leaf senescence-associated genes. *The Plant Journal* **36**: 629–642.

Gonzales LYRR. 2022. *Linking plant development and tuberization: to key environmental inputs of light, water and nitrogen in potato*. PhD thesis, Wageningen University, Wageningen, the Netherlands.

Guiboileau A, Sormani R, Meyer C, Masclaux-Daubresse C. 2010. Senescence and death of plant organs: nutrient recycling and developmental regulation. *Comptes Rendus Biologies* **333**: 382–391.

Guzzo MC, Costamagna C, Salloum MS, Rotundo JL, Monteoliva MI, Luna CM. 2021. Morpho-physiological traits associated with drought responses in soybean. *Crop Science* **61**: 672–688.

Hoeberichts FA, van Doorn WG, Vorst O, Hall RD, van Wordragen MF. 2007. Sucrose prevents up-regulation of senescence-associated genes in carnation petals. *Journal of Experimental Botany* **58**: 2873–2885.

Hoopes G, Meng X, Hamilton JP, Achakkagari SR, Guesdes FAF, Bolger ME, Coombs JJ, Esselink D, Kaiser NR, Kodde L. 2022. Phased, chromosome-scale genome assemblies of tetraploid potato reveal a complex genome, transcriptome, and predicted proteome landscape underpinning genetic diversity. *Molecular Plant* **15**: 520–536.

Horacio P, Martinez-Noel G. 2013. Sucrose signaling in plants: a world yet to be explored. *Plant Signaling & Behavior* **8**: e23316.

Hörtensteiner S. 2009. Stay-green regulates chlorophyll and chlorophyll-binding protein degradation during senescence. *Trends in Plant Science* **14**: 155–162.

Hurtado PX, Schnabel SK, Zaban A, Veteläinen M, Virtanen E, Eilers PHC, van Eeuwijk FA, Visser RGF, Maliepaard C. 2011. Dynamics of senescence-related QTLs in potato. *Euphytica* **183**: 289–302.

Jing S, Sun X, Yu L, Wang E, Cheng Z, Liu H, Jiang P, Qin J, Begum S, Song B. 2022. Transcription factor StABI5-like 1 binding to the FLOWERING LOCUS T homologs promotes early maturity in potato. *Plant Physiology* **189**: 1677–1693.

Joshi S, Choukimath A, Isenegger D, Panozzo J, Spangenberg G, Kant S. 2019. Improved wheat growth and yield by delayed leaf senescence using developmentally regulated expression of a cytokinin biosynthesis gene. *Frontiers in Plant Science* **10**: 1285.

Kamranfar I, Xue GP, Tohge T, Sedaghatmehr M, Fernie AR, Balazadeh S, Mueller-Roeber B. 2018. Transcription factor RD 26 is a key regulator of metabolic reprogramming during dark-induced senescence. *New Phytologist* **218**: 1543–1557.

Kim H, Kim HJ, Vu QT, Jung S, McClung CR, Hong S, Nam HG. 2018. Circadian control of ORE1 by PRR9 positively regulates leaf senescence in Arabidopsis. *Proceedings of the National Academy of Sciences, USA* **115**: 8448–8453.

Kim JH, Woo HR, Kim J, Lim PO, Lee IC, Choi SH, Hwang D, Nam HG. 2009. Trifurcate feed-forward regulation of age-dependent cell death involving miR164 in Arabidopsis. *Science* **323**: 1053–1057.

Kleinwechter U, Gastelo M, Ritchie J, Nelson G, Asseng S. 2016. Simulating cultivar variations in potato yields for contrasting environments. *Agricultural Systems* **145**: 51–63.

Kloosterman B, Abelenda JA, Gomez Mdel M, Oortwijn M, de Boer JM, Kowitwanich K, Horvath BM, van Eck HJ, Smaczniak C, Prat S *et al.* 2013. Naturally occurring allele diversity allows potato cultivation in northern latitudes. *Nature* **495**: 246–250.

Li J, Wang Y, Wen G, Li G, Li Z, Zhang R, Ma S, Zhou J, Xie C. 2019. Mapping QTL underlying tuber starch content and plant maturity in tetraploid potato. *The Crop Journal* **7**: 261–272.

Li W, Liu Y, Liu M, Zheng Q, Li B, Li Z, Li H. 2019. Sugar accumulation is associated with leaf senescence induced by long-term high light in wheat. *Plant Science* **287**: 110169.

Lightenthaler H. 1987. Chlorophylls and carotenoids: pigments of photosynthetic biomembranes. *Methods in Enzymology* **148**: 350–382.

Lira BS, Gramegna G, Trench BA, Alves FR, Silva EM, Silva GF, Thirumalaikumar VP, Lupi AC, Demarco D, Purgatto E. 2017. Manipulation of a senescence-associated gene improves fleshy fruit yield. *Plant Physiology* **175**: 77–91.

Lohman KN, Gan S, John MC, Amasino RM. 1994. Molecular analysis of natural leaf senescence in Arabidopsis thaliana. *Physiologia Plantarum* **92**: 322–328.

Ma X, Zhang Y, Turečková V, Xue G-P, Fernie AR, Mueller-Roeber B, Balazadeh S. 2018. The NAC transcription factor SlNAP2 regulates leaf senescence and fruit yield in tomato. *Plant Physiology* **177**: 1286–1302.

Manrique-Carpintero NC, Coombs JJ, Cui Y, Veilleux RE, Buell CR, Douches D. 2015. Genetic map and QTL analysis of agronomic traits in a diploid potato population using single nucleotide polymorphism markers. *Crop Science* **55**: 2566–2579.

Marand AP, Jansky SH, Gage JL, Hamernik AJ, de Leon N, Jiang J. 2019. Residual heterozygosity and epistatic interactions underlie the complex genetic architecture of yield in diploid potato. *Genetics* **212**: 317–332.

Matallana-Ramirez LP, Rauf M, Farage-Barhom S, Dortay H, Xue G-P, Dröge-Laser W, Lers A, Balazadeh S, Mueller-Roeber B. 2013. NAC transcription factor ORE1 and senescence-induced BIFUNCTIONAL NUCLEASE1 (BFN1) constitute a regulatory cascade in Arabidopsis. *Molecular Plant* **6**: 1438–1452.

Maul F, Sargent SA, Balaban MO, Baldwin EA, Huber DJ, Sims CA. 1998. Aroma volatile profiles from ripe tomatoes are influenced by physiological maturity at harvest: an application for electronic nose technology. *Journal of the American Society for Horticultural Science* **123**: 1094–1101.

Moore B, Zhou L, Rolland F, Hall Q, Cheng W-H, Liu Y-X, Hwang I, Jones T, Sheen J. 2003. Role of the Arabidopsis glucose sensor HXK1 in nutrient, light, and hormonal signaling. *Science* **300**: 332–336.

Navarro C, Abelenda JA, Cruz-Oró E, Cuéllar CA, Tamaki S, Silva J, Shimamoto K, Prat S. 2011. Control of flowering and storage organ formation in potato by FLOWERING LOCUS T. *Nature* **478**: 119–122.

Park BS, Yao T, Seo JS, Wong ECC, Mitsuda N, Huang C-H, Chua N-H. 2018. Arabidopsis NITROGEN LIMITATION ADAPTATION regulates ORE1 homeostasis during senescence induced by nitrogen deficiency. *Nature Plants* **4**: 898–903.

Pourtau N, Jennings R, Pelzer E, Pallas J, Wingler A. 2006. Effect of sugar-induced senescence on gene expression and implications for the regulation of senescence in Arabidopsis. *Planta* **224**: 556–568.

Prat S. 2006. Seasonal control of tuberization in potato: conserved elements with the flowering response. *Annual Review of Plant Biology* **57**: 151–180.

Pulido A, Laufs P. 2010. Co-ordination of developmental processes by small RNAs during leaf development. *Journal of Experimental Botany* **61**: 1277–1291.

Qiu K, Li Z, Yang Z, Chen J, Wu S, Zhu X, Gao S, Gao J, Ren G, Kuai B *et al.* 2015. EIN3 and ORE1 accelerate degreening during ethylene-mediated leaf senescence by directly activating chlorophyll catabolic genes in Arabidopsis. *PLoS Genetics* **11**: e1005399.

Ramírez Gonzales L, Shi L, Bergonzi SB, Oortwijn M, Franco-Zorrilla JM, Solano-Tavira R, Visser RG, Abelenda JA, Bachem CW. 2021. Potato CYCLING DOF FACTOR 1 and its lncRNA counterpart StFLORE link tuber development and drought response. *The Plant Journal* **105**: 855–869.

Rauf M, Arif M, Dortay H, Matallana-Ramírez LP, Waters MT, Gil Nam H, Lim PO, Mueller-Roeber B, Balazadeh S. 2013. ORE1 balances leaf senescence against maintenance by antagonizing G2-like-mediated transcription. *EMBO Reports* **14**: 382–388.

Stöckle CO, Nelson RL, Higgins S, Brunner J, Grove G, Boydston R, Whiting M, Kruger C. 2010. Assessment of climate change impact on Eastern Washington agriculture. *Climatic Change* **102**: 77–102.

TeKrony D, Egli D, Balles J, Pfeiffer T, Fellows R. 1979. Physiological maturity in soybean 1. *Agronomy Journal* **71**: 771–775.

Teo C-J, Takahashi K, Shimizu K, Shimamoto K, Taoka K-i. 2017. Potato tuber induction is regulated by interactions between components of a tuberigen complex. *Plant and Cell Physiology* **58**: 365–374.

Visker M, Keizer L, Van Eck H, Jacobsen E, Colon L, Struik P. 2003. Can the QTL for late blight resistance on potato chromosome 5 be attributed to foliage maturity type? *Theoretical and Applied Genetics* **106**: 317–325.

Visser RGF, Hesseling-Meinders A, Jacobsen E, Nijdam H, Witholt B, Feenstra WJ. 1989. Expression and inheritance of inserted markers in binary vector carrying *Agrobacterium rhizogenes* transformed potato (*Solanum tuberosum* L.). *Theoretical and Applied Genetics* **78**: 705–714.

Wallace D, Baudoin J, Beaver J, Coyne D, Halseth D, Masaya P, Munger H, Myers J, Silbernagel M, Yourstone K. 1993. Improving efficiency of breeding for higher crop yield. *Theoretical and Applied Genetics* **86**: 27–40.

Wang G, Wang C, Lu G, Wang W, Mao G, Habben JE, Song C, Wang J, Chen J, Gao Y. 2020. Knockouts of a late flowering gene via CRISPR–Cas9 confer early maturity in rice at multiple field locations. *Plant Molecular Biology* **104**: 137–150.

Wingler A. 2018. Transitioning to the next phase: the role of sugar signaling throughout the plant life cycle. *Plant Physiology* **176**: 1075–1084.

Woo HR, Kim JH, Nam HG, Lim PO. 2004. The delayed leaf senescence mutants of Arabidopsis, ore1, ore3, and ore9 are tolerant to oxidative stress. *Plant and Cell Physiology* **45**: 923–932.

Woo HR, Masclaux-Daubresse C, Lim PO. 2018. *Plant senescence: how plants know when and how to die.* Oxford, UK: Oxford University Press, 715–718.

Xujun W, Qingguo X, Zhijian Y. 2005. Advances of research on rice leaf senescence physiology. *Zhongguo Nong xue Tong bao= Chinese Agricultural Science Bulletin* **21**: 187.

Yang S, Fang G, Zhang A, Ruan B, Jiang H, Ding S, Liu C, Zhang Y, Jaha N, Hu P. 2020. Rice EARLY SENESCENCE 2, encoding an inositol polyphosphate kinase, is involved in leaf senescence. *BMC Plant Biology* **20**: 1–15.

Yuan J, Murphy A, De Koeyer D, Lague M, Bizimungu B. 2016. Effectiveness of the field selection parameters on potato yield in Atlantic Canada. *Canadian Journal of Plant Science* **96**: 701–710.

Zaheer K, Akhtar MH. 2016. Potato production, usage, and nutrition—a review. *Critical Reviews in Food Science and Nutrition* **56**: 711–721.

Zhang X, Campbell R, Ducreux LJ, Morris J, Hedley PE, Mellado-Ortega E, Roberts AG, Stephens J, Bryan GJ, Torrance L. 2020. TERMINAL FLOWER-1/CENTRORADIALIS inhibits tuberisation via protein interaction with the tuberigen activation complex. *The Plant Journal* **103**: 2263–2278.

Zhang Y, Gao Y, Wang H-L, Kan C, Li Z, Yang X, Yin W, Xia X, Nam HG, Li Z. 2021. *Verticillium dahliae* secretory effector PevD1 induces leaf senescence by promoting ORE1-mediated ethylene biosynthesis. *Molecular Plant* **14**: 1901–1917.

Zhaowei L, Qian Z, Fangmin C. 2020. Sugar starvation enhances leaf senescence and genes involved in sugar signaling pathways regulate early leaf senescence in mutant rice. *Rice Science* **27**: 201–214.

Supporting Information

Additional Supporting Information may be found online in the Supporting Information section at the end of the article.

Fig. S1 Knocking down StCDF1 in CE3130 leads to extended life cycle length.

Fig. S2 DNA and protein sequence alignments of *StCDF1.2* and *StCDF1.2*^{Coed}.

Fig. S3 Characterization of transgenic potato plants overexpressing *StCDF1.2*^{Coed}.

Fig. S4 Transient dual-luciferase reporter assay.

Fig. S5 Log scale of the relative expression of StORE1S02 for the first 3 wk of sample harvesting.

Fig. S6 Alignments of *StORE1* genes and the RNAi targeting region.

Fig. S7 Log scale of the relative expression of *StSP6A* in *StORE1S02* knockdown and overexpressing plants at 37DAP.

Fig. S8 Glucose content in leaves of CE3130 and StORE1S02 knockdown lines in CE3130 background (KD #3 and KD #4) at different time points (23, 30, 37 and 43 d after plant, DAP).

Fig. S9 Relative expression of the *StSAG29/SWEET15* in CE3130 background (KD #3 and KD #4) at different time points (23, 30, 37 and 43 DAP).

Fig. S10 Transient assay to test the activation of pStSWEET11:: iLUC luciferase activity by 35S::*StORE1S02* in *Nicotiana benthamiana* leaves.

Fig. S11 Relative expression of the *StHXK1* in the same samples as in CE3130 and *StORE1S02* knockdown lines in CE3130 background (KD #3 and KD #4) at 37 DAP.

Table S1 Specific primer pairs for qRT-PCR reaction.

Table S2 Statistical analysis for Fig. 1(e).

Table S3 ORE1 homologs in 13 plant species.

Please note: Wiley is not responsible for the content or functionality of any Supporting Information supplied by the authors. Any queries (other than missing material) should be directed to the *New Phytologist* Central Office.